2016

The Behavior of Simply Supported Plates under Extreme Shear Loading

Mhd ammar Hafez

THE BEHAVIOR OF SIMPLY SUPPORTED PLATES UNDER EXTREME SHEAR LOADING

MHD AMMAR HAFEZ

Bachelor in Civil Engineering
at Damascus University
2012

Submitted in partial fulfillment of requirements for the degree
MASTER OF SCIENCE IN CIVIL ENGINEERING
At the
CLEVELAND STATE UNIVERSITY
DECEMBER 2016

We hereby approve thesis

of

MHD AMMAR HAFEZ

Candidate for the Masters of Civil Engineering degree.

This thesis has been approved

For the Department of

Civil and Environmental Engineering

And

CLEVELAND STATE UNIVERSITY

College of Graduate Studies by

Dr. Mehdi Jalalpour

Department & Date

Dr. Lutful I. Khan

Department & Date

Dr. Stephen F. Duffy

Department & Date

Dec. 7th, 2016

Student's Date of Defense

ACKNOWLEDGEMENTS

After thanking Allah for giving me the chance to purse my graduate studies. I want to thank Dr. Mehdi Jalalpour for his care, guidence, and helping me develop my research skills. Dr. Jalalpour has been always generous with his knowledge and instruction through both advising in this thesis and during the courses he tought me. Also, I want to thank both Dr. Stephen Duffy and Dr. Lutful Khan for their time reading this thesis and their comments that helped improve this thesis.

This thesis is dedicated to my Parents, Shaza, my country Syria and its martyrs.

THE BEHAVIOR OF SIMPLY SUPPORTED PLATES UNDER EXTREME SHEAR LOADING

MHD AMMAR HAFEZ

ABSTRACT

Steel plates are planar structural elements with one dimension significantly smaller than the others. These elements may fail due to either material yielding or buckling. Buckling is a sudden failure mode, which is not desirable in structural engineering applications. Buckling is called an “elastic buckling” when it happens before material yielding, and is termed as “plastic buckling” if it happens after material yielding. The focus of this thesis is on shear plates, which are plates that are primarily subjected to shear loads. Several studies were conducted to increase the elastic buckling capacity of plates by adding stiffeners to plates. However, the research appears inconclusive as to whether the overall behavior of the plate will change so that buckling will happen after yielding (i.e., changing elastic buckling to plastic buckling).

The aim of this thesis was to analyze the performance of simply supported shear plates with and without stiffeners and determine whether a behavior change is possible by adding stiffeners. For this purpose, a variety of plates were studied by measuring the elastic critical buckling load and the yielding load to evaluate plate performance. A

parametric study was conducted with varying plate slenderness ratio, initial imperfection magnitude and pattern, and number and the arrangement of the stiffeners. This resulted in 42 separate plate models that were analyzed using a non-linear finite element analysis with the ABQUS software. It was found that adding stiffeners to a steel plate can change plate overall behavior. This is manifested by reducing the difference between the elastic critical buckling load and the yielding load until buckling load is greater than yield load, which changes the plate behavior from slender to stocky plate. Furthermore, it was found that stiffener design is a critical criterion. Overdesigning stiffeners may lead to local yielding in plates which precludes the attainment of the intended capacity.

TABLE OF CONTENTS

LIST OF FIGURES

LIST OF TABLES

CHAPTER I

INTRODUCTION

Structural steel plates are planar bodies that have thicknesses significantly smaller than the other dimensions. Shear plates (plates that primarily transfer shear loads) are widely used in civil, naval and aeronautical engineering. Design of these plates is generally based on material yielding and geometrical buckling modes of failure. Buckling is an instability mode of failure that is caused by an excessive compression stress, and results in a sudden out-of-plane deformation of the plate. We note that in simply supported plates under pure shear, a tension and compression diagonal fields appear, and buckling happens due to the diagonal compression field stresses. Depending on the plate material properties, aspect ratio and boundary conditions yielding may occur before, after or at the same time as buckling. Because buckling is generally a sudden mode of failure, it is desirable to delay buckling to after material yielding. Therefore, plates are divided into slender and stocky groups based on their buckling and yielding strength. A moderate plate category, which is a transitional state from slender to stocky, could also be defined. Buckling in slender plates happens prior to yielding (elastic buckling), and is a local and

sudden phenomenon followed by large out-of-plane displacements and loss of stiffness. Stocky plates, on the other hand, yield before buckling and fail due to excessive deformation or material yielding, which is termed as plastic buckling (Alinia et al. 2009). Stocky plates are mainly used in bridge plate girders, liquid and gas container structures, shelters, offshore structures, ship structures, slabs, some of the hot-rolled W-shape steel sections and steel plate shear wall buildings, while thin plates are used in, for example, aeronautical engineering structures. The behavior of plates was investigated intensively using analytical (mathematical equations), numerical (primarily finite-element analysis) and experimental methods. We restrict the following discussion to the analytical and numerical studies.

It is well-known that plate boundary conditions are important in determining the buckling capacity. The primary limiting boundary conditions are simply supported and clamped, where the out-of-plane rotations are free in the former and are completely restrained in the latter. Initial analytical studies only considered these limiting boundary conditions under elastic material behavior and simple loads. For example, (Tetsuro & Ben 1993), theoretically obtained buckling stress of simply supported rectangular steel shear plates. Plate yielding followed the Tresca yield criterion and plastic deformation seemed to be caused by slips which developed only in the direction of maximum shear stress. Later on, (Wang et al. 2001) presented the elastic/plastic buckling equations for thick plates under (a) uniaxially and equibiaxially (with equal magnitudes) loaded rectangular plates with two opposite edges simply supported while the other two edges might took on any combination of free, simply supported or clamped boundary condition

and (b) uniformly in-plane loaded circular plates with either simply supported edge or clamped edge. The Mindlin plate theory was adopted to admit the effect of transverse shear deformation, which becomes significant in thick plates. They considered two competing plasticity theories: the incremental theory of plasticity (IT) with the Prandtl-Reuss constitutive equations and the deformation theory of plasticity (DT) with the Hencky constitutive equations. The stability for uniaxially loaded and equibiaxially loaded rectangular plates and uniform radially loaded circular plates was investigated, which resulted in extensive closed-form equations for buckling stresses. Moreover, (Wang et al. 2004) presented an analytical method for determining the exact plastic buckling factors of rectangular plates subjected to end and intermediate uniaxial loads, and where two opposite edges (parallel to the loads) of the plates were simply supported. In this method, the rectangular plate was divided into two sub plates at the intermediate load location. Each sub-plate buckling problem was then solved using the Levy approach. Therefore, eight feasible solutions for each sub-plate were derived. The critical buckling load was determined from one of the 64 possible solution combinations for the two sub-plates. The solution combination depended on the aspect ratio, the intermediate load position, the intermediate to end load ratio, the material properties and the boundary conditions.

Under complex boundary conditions and loads, studying plate behavior analytically becomes complicated if not impossible. Moreover, it is of interest to analyze the plastic buckling regime of plates. Therefore, finite-element method (FEM) is a prominent method to numerically study the plate behavior (using linear and nonlinear analysis). As

an example of application of FEM to complex boundary conditions, we mention the work of (Alinia & Dastfan 2006) where they study the effects of surrounding members (i.e. beams and columns) on the overall behavior of thin steel plate shear walls. They find out that shear walls that are surrounded by beams and columns should not be considered as simply supported. The torsional stiffness of supporting members is highly effective in increasing the elastic buckling load, but it does not affect the post-buckling strength (the behavior after reaching the buckling critical load).

(Alinia et al. 2009) used slenderness ratio, which they defined as smaller plate dimension over its thickness, to classify shear plates. They examined plastic buckling (under the action of pure in-plane shear loads). They concluded that flat plates in accordance with their slenderness ratios can be qualitatively divided into three categories:

- Slender plates: have small buckling capacity, followed by large out-of-plane deformations and post buckling (the behavior of plate after buckling critical load) reserves. Their ultimate loads coincide with the formation of inclined yield zones.
- Stocky plates: yield before buckling. They have some post-yield capacity prior to plastic buckling. This post-yield capacity primarily depends on the strain hardening moduli of elasticity.
- Moderate plates: have concurrent material yielding and geometrical buckling followed by considerable stiffness loss and softening.

However, (Gheitasi & Alinia 2010) used a slenderness parameter to classify shear plates with several material types (carbon steel, stainless steel and aluminum). Their slenderness parameters was defined as follows:

$$\lambda = \beta\sqrt{\frac{\sigma_y}{E}} \qquad (1)$$

where β was the slenderness ratio.

They found that plates with $\lambda \geq 6$ buckle at relatively small shear loads and their ultimate strength, which occurs during post buckling action is much less than the yield load. Slender plates bifurcated (when the load-deflection curve had more than one possible path) due to geometrical instability within the elastic limits. They concluded that concurrent geometrical and material bifurcations governed moderate plates. These plates had neither post buckling nor post-yield reserves. The bifurcation point and the post-bifurcation behavior of stocky shear, with a slenderness parameter of less than 4.5, were directly affected by the presumed material stress–strain relationship. The onset of material nonlinearity, characterized by the proportional limit stress, was the bifurcation point of stocky plates. (Amani et al. 2013) classified unstiffened mild carbon steel, stainless steel and aluminum plates under the action of axial compression according to their slnderness parameter. Because the buckling mode of failure is caused by an initial imperfection in the plate, they studied the effects of initial imperfection amplitude on each plate type and material. They found out that a slender plate was characterized as having a slenderness parameter of greater than 2. Elastic buckling occured in slender plates, and they had significant post buckling reserves, which increased linearly with the slenderness parameter. Stocky plates had slenderness parameters of less than 2 and buckling coefficient of stocky plates varied considerably with the slenderness parameter. Stocky plates underwent inelastic buckling, and had equal buckling and ultimate loads. These plates had some post-yield capacity which increased with the plate thickness. In

addition, they derived empirical equations for evaluating buckling and post buckling capacities of plates with geometric imperfections. They showed that the increase of imperfection amplitude decreased the buckling load of slender plates, but their post buckling reserves and ultimate capacities were unaffected. However, they concluded that the ultimate strength of stocky plates was very sensitive to initial imperfections.

Plates could be stiffened for improving their load-bearing behavior. Stiffening means attaching plates perpendicular to the thin dimension of the plate (usually through welding). (Sanal & Gunay 2008) presented a finite element buckling analyses of transversely stiffened isotropic and orthotropic rectangular slender plates under shear loads. They found that by increasing the height of the stiffeners, the critical buckling stresses of the stiffened plates increase. With the addition of the transverse stiffeners to the plates their critical buckling stresses increase linearly.

(Alinia & Sarraf Shirazi 2009) described a numerical investigation to provide a practical design method for stiffening thin steel plate shear walls. They considered one-sided transverse and longitudinal flat stiffeners in various arrangements. They suggested that these stiffeners effectively divided the plate into subpanels and expanded tension fields across the infill shear walls. Several interesting findings resulted from their study. First, they suggested that thin unstiffened steel shear panels had a ductile behavior (less rigid and allowed deformation in early stages after applying loads) and buckled early. Second, stiffeners could protect the shear walls against overall buckling, limited their out-of-plane deflections, increased their elastic buckling strength, and extended yielding throughout the plate. They also suggested that in an optimal stiffener arrangement, the critical

stresses of stiffened plates were equal to the critical stresses of individual subpanels. Finally, they developed empirical relationships for evaluating optimal dimensions of stiffeners, and showed that the optimal thickness and height of stiffeners seemed to be related to each other and to the plate dimensions. Nonlinear analyses showed that the post buckling reserves of plates having different optimized stiffeners were very similar. Also, the initial stiffness of plates having various optimal stiffeners was identical; but once they buckled, their stiffness gradually decreased with the loading. Increasing the number of stiffeners made the walls more rigid and less ductile. More importantly, their results showed that utilizing unidirectional stiffeners were more effective than bidirectional cross stiffeners. (Zirakian & Zhang 2015) studied low yield point (LYP) steel plates under various support and loading conditions (static and cyclic loading) for application in steel plate shear wall (SPSW) systems. They found that plates with two clamped-two free edges, representing beam-attached infill plates in SPSW systems, exhibited relatively weak performance because of excessive out-of-plane deformations due to presence of the two unrestrained edges. The cyclic performance of such (beam-attached) plates could be significantly improved by limiting the plate out-of- plane deformations through strategic placement of stiffeners. It was shown that using LYP steel, compared to conventional steel, reduced the required limiting plate thickness considerably. Moreover, their results suggested that unstiffened plates with higher length-to-height ratio may require larger limiting plate thickness.

The literature surveyed above shows that a wealth of research exists on the behavior of thin and stocky plates, and adding the stiffeners improves the plate buckling loads.

However, no research has explored the possibility of changing the overall behavior of a plate from slender to stocky through adding stiffeners. This is important as plate failure will be due to material yielding, and not because of buckling, which is a sudden failure mode. The aim of this thesis is to numerically investigate if the thin plate behavior can be changed by adding stiffeners. This thesis is structured as follows: in Chapter II, the finite element model and plate material is described. Also, a verification of the nonlinear finite element analysis is presented. Chapter III implements a parametric design and presents results for several cases and a discussion of the results. Chapter IV presents conclusions and future research recommendations.

CHAPTER II

METHODS

In this chapter, we described the material properties, plate geometry and boundary conditions, stiffeners arrangement and the details of the implemented finite element model.

2.1 Material properties:

The material used in plates of this study was a mild steel (low carbon) with a yield stress of 345 MPa similar to (Alinia & Sarraf Shirazi 2009). This material was modeled using a bi-linear elasto-plastic model. Table 1 shows the material properties:

Table 1: Materials properties

σ_y	ν	E_1	E_2
345 Mpa	0.3	210 GPa	2.1 GPa

where ν, σ_y, E are the material Poisson ratio, yield stress and Young's modulus respectively. The stress-strain relationship model is also plotted in Figure 1.

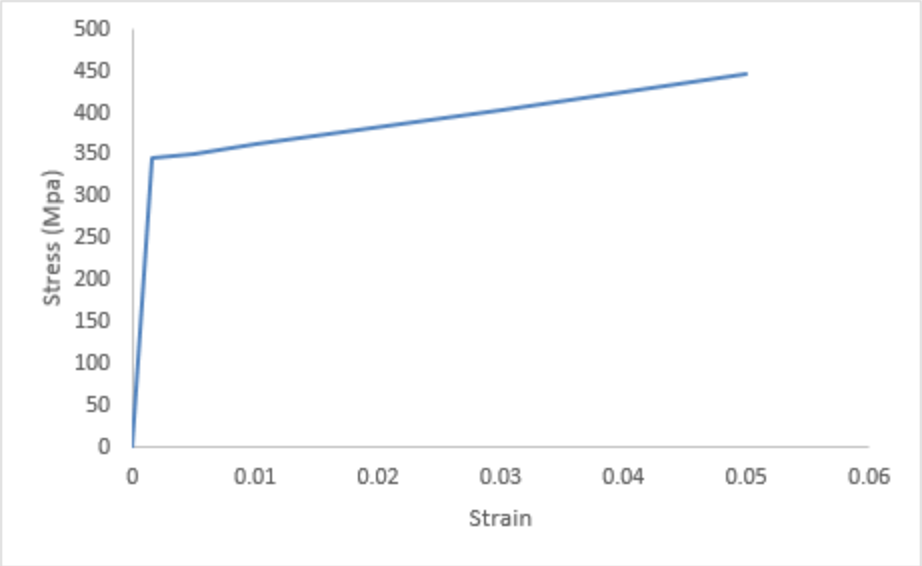

Figure 1. Stress versus strain relation for the steel used

2.2 Plate's geometry:

Square plates with dimensions of $1000\times1000\ mm^2$, were used in this study. Figure 2 shows the boundary conditions used in the study. These boundary conditions were set so that under the applied shear loads on all sides, the plate behaved as close as possible to a state of pure shear.

Edge No.	U_x	U_y	U_z	R_x	R_y	R_z
1	0	0	1	0	0	1
2	0	0	1	0	0	1
3	1	1	1	0	0	1
4	0	0	1	0	0	1

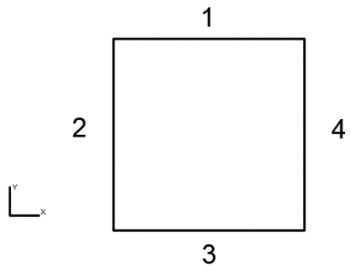

Figure 2: Boundary conditions for the simply supported plate

2.3 Elastic buckling critical load (P_{cr}):

For verification of the FEM results, the elastic buckling critical load was calculated theoretically using the following classical equation:

$$P_{cr} = \tau_{cr} * b * t \qquad (2)$$

where τ_{cr} is the elastic buckling shear stress which is calculated as follows (Alinia & Sarraf Shirazi 2009):

$$\tau_{cr} = k_s \frac{\pi^2 * E}{12*(1-\nu^2)} * (\frac{t_b}{b})^2 \qquad (3)$$

where t_b is the plate thickness, a, b are the plate dimensions, and k_s is the elastic shear buckling coefficient. For simply supported plates, we have: $k_s = 5.34 + 4 * (\frac{a}{b})^2$.

2.4 Von Mises yield criterion:

Materials yield according to von Mises when:

$$J_2 = K^2 \qquad (4)$$

where J_2 is the second invariant in stress deviator and $K = \frac{\sigma_y}{3}$. Yield load (P_y) was calculated theoretically using the von Mises criterion which is accurate in predicting the initiation of yielding for most of the ductile metals. Moreover, it is more accurate than the Tresca criterion in predicting yield under pure shear (Gerstle 2001). The plates in this study were subjected to (approximately) a state of pure shear $\sigma_1 = -\sigma_2 = \sigma, \sigma_3 = 0$. Therefore, according to von Mises:

$$\tau_y = \frac{\sigma_y}{\sqrt{3}} \qquad (5)$$

where τ_y is the yield shear stress, and we have:

$$P_y = \tau_y * b * t_b \qquad (6)$$

We note, however, that due to stress concentrations in the corners of the plate, local yielding may happen in these places before actual yielding of the plate. We therefore, neglect these local yileding in all the following discussions. This resulted in a very close match between theroetical and the FEM results for the cases where analytical equations were available.

2.5 Slenderness ratio (β):

This ratio is used in (Zirakian & Zhang 2015) and is defined as follows:

$$\beta = \frac{b}{t_b} \qquad (7)$$

The higher this ratio is, the thicker is the plate, and it is more likely to be classified as stocky (see next chapter).

2.6 Stiffeners design:

In this thesis, we adopt the following notation for showing the stiffeners arrangement: $xHyV$, where x shows the number of stiffeners in the horizontal direction and y shows the number of stiffeners in vertical direction. We follow (Alinia & Sarraf Shirazi 2009) for designing stiffeners thickness t_s and height h_s to limit the stiffeners local buckling. It is noted that they used the AASHTO provisions for the projecting width of the transverse stiffeners of steel plate girders, which are given in Eq. (8) and (9). The thickness of the stiffener was further limited by the weldability of material, and it was assumed that:

$$t_p \leq t_s < 5t_p \qquad (8)$$

$$\frac{h_s}{t_s} \leq 0.48\sqrt{\frac{E}{\sigma_y}} \qquad (9)$$

The following stiffener arrangement cases will be discussed. In each case, the recommended design equation is presented as well.

-A single central horizontal stiffener ($1H0V$):

$$t_s {h_s}^2 \geq 0.7 {t_p}^2 b \qquad (10)$$

-Multiple equally spaced horizontal stiffeners ($xH0V$):

$$t_s {h_s}^2 \geq 0.7\left(1+\frac{2x}{10}\right){t_p}^2 b, x > 1 \qquad (11)$$

- A single horizontal and vertical cross stiffeners ($1H1V$):

$$t_s {h_s}^{2.5} \geq 1.8 {t_p}^{2.5} b \qquad (12)$$

- Multiple equally spaced horizontal and vertical cross stiffeners ($xHyV$):

$$t_s {h_s}^{2.5} \geq 1.8\left(1+\frac{x}{10}\right) {t_p}^{2.5} b, x > 1 \quad (13)$$

2.7 Finite Element Analysis:

Nonlinear finite element analysis software Abaqus (V. 6.14) was used in this study. Both plates and the stiffeners were modeled by the element S4R which is a 4-node, quadrilateral, stress/displacement shell element with reduced integration and large strain formulations. This element has six degrees of freedom per node ($U_x, U_y, U_z, R_x, R_y, R_z$). Figure 3 shows the S4R element.

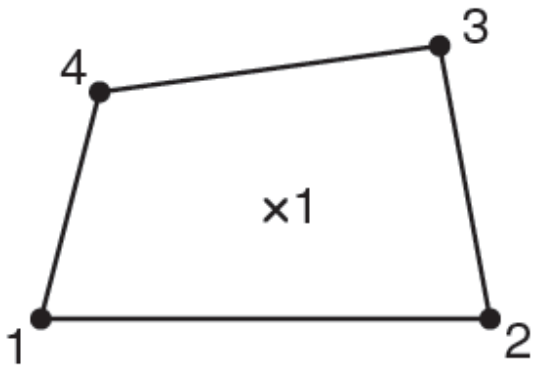

Figure 3: 4 - node reduced integration element

The nonlinearity in the model included both geometric nonlinearities and plate material property nonlinearities. $20\times20\ mm^2$ elements were used in the simulation, which gave a good convergence for the models. Table 6 shows P_{cr} values from both finite element analysis using $20\times20\ mm^2$ elements and P_{cr} from Eq. (2).

2.8 Riks Analysis:

2.8.1 Introduction:

In this thesis, Riks analysis is used to determine the yield load for unstiffened and stiffened plates. This method is generally used to predict unstable, geometrically nonlinear collapse of a structure (Abaqus 6.12: Analysis User's Manual Volume 2: Analysis 2012).

The Riks method uses the load magnitude as an additional unknown; it solves simultaneously for loads and displacements. Therefore, another quantity must be used to measure the progress of the solution; Abaqus uses the "arc length," l, along the static equilibrium path in the load-displacement space. This approach provides solutions regardless of whether the response is stable or unstable. Before using this method extensively, we briefly verify the Abaqus implementation in the next subsection using the defined square plate with $1000\ mm$ dimensions.

2.8.2 Validation of buckling loads:

To validate the implemented Riks analysis in predicting the buckling load, a square plate with $t = 2\ mm$ was studied. No initial imperfection was applied so the buckle load will not be reduced due to the imperfection. Eq.(2) and (3) yield the following elastic critical buckling load:

$\tau_{cr} = 7.1\ MPa$ and $P_{cr} = 14.2\ KN$.

Figure 4 shows the force versus out-of-plane displacement and the stress distribution for the plate when buckling started using Riks analysis. From Figure 4, we conclude that the buckling happened at force $F = 14.9\ KN$. This is because at this force magnitude, the plate continues to deform without a large load increment, which suggest that at this point

buckling happens. Moreover, the von Mises stress distribution at this load magnitude, which is shown in the bottom panel of Figure 4, indicates no yielding in the material. Therefore, the excessive displacements are likely due to buckling. Because the difference between the load from the analysis and the load from Eq. (2) is less than 5%, the Riks analysis appears to predict the buckling load with a good accuracy.

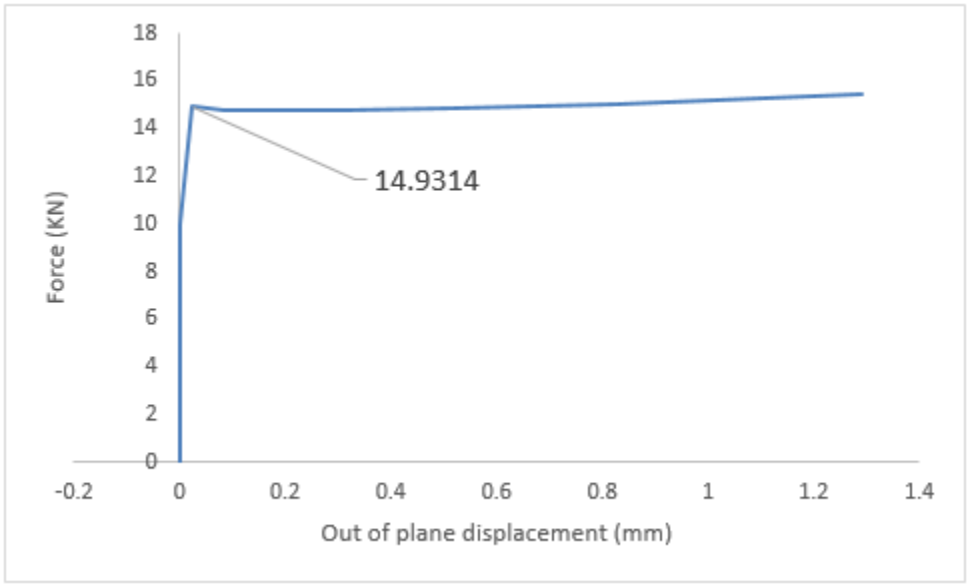

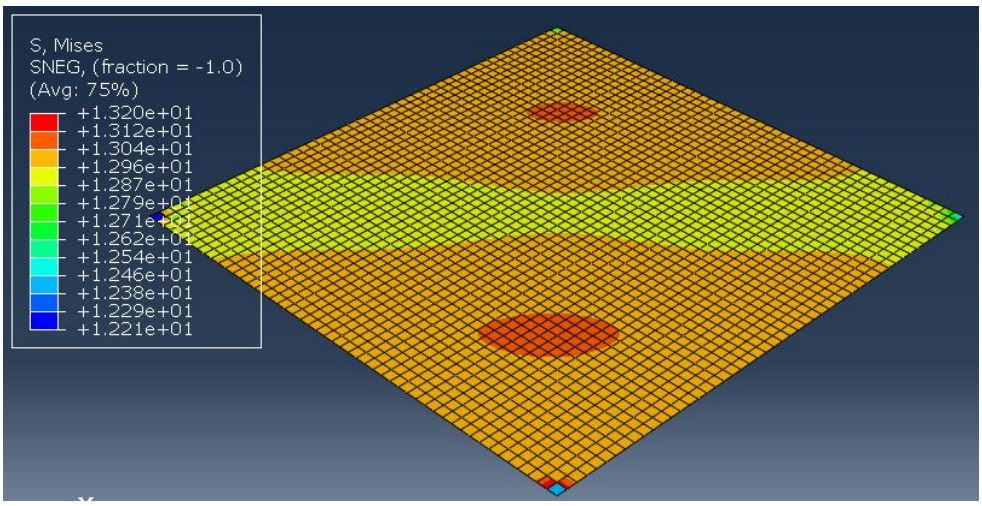

Figure 4: Force-out of plane displacement plot and the stress distribution at the buckling state

2.8.3 Validation for yield loads:

To validate the Riks analysis in predicting the yielding load. A thicker plate with thickness ($12\ mm$) was studied. Eqs. (5) and (6) give the following analytical results for yield stress and loads:

$$\tau_y = 199.19, Mpa \text{ and } P_y = 2390.23\ Mpa$$

Figure 5 shows the force vs out-of-plane displacement curve for the plate using resulted from the FEM. From this Figure and by using von Mises criterion we conclude that yield load $P_y^{FEM} = 2395.07$ KN. The difference between the load from the implemented Riks analysis and analytical results is less than 5%, which verifies the numerical model.

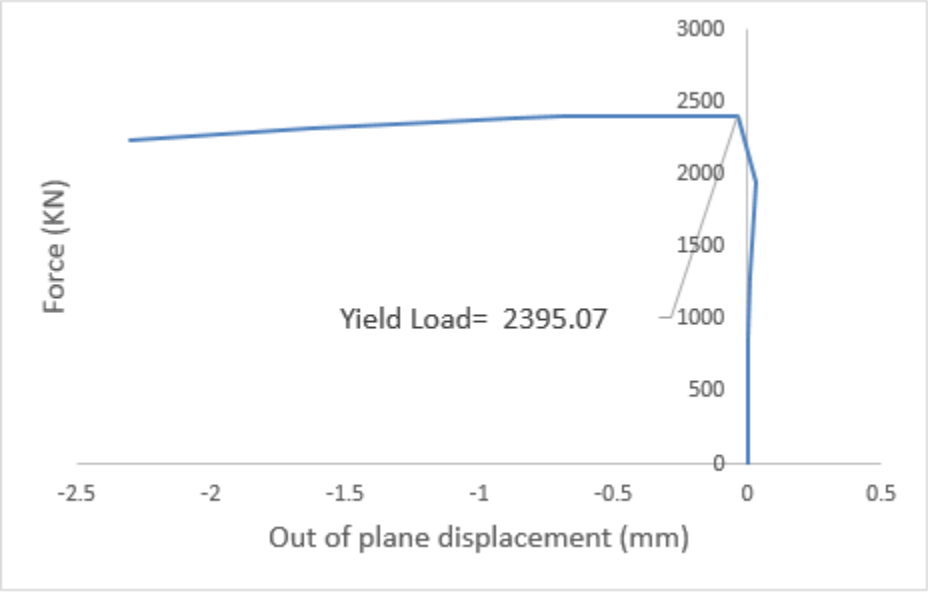

Figure 5: Force vs out-of-plane displacement for the test case

CHAPTER III

PARAMETRIC STUDY

In this chapter, two sets of plates are analyzed using the numerical model described in the previous chapter: 1) plates without stiffeners, and 2) stiffened plates.

3.1 Plates without stiffeners:

3.1.1 Plate geometry:

As mentioned previously, all plates have dimensions of $1000\times1000\ mm^2$. Here we vary the plate thickness t, which in turn changes the slenderness parameter β, which is defined previously in Eq.(7). Table 2 shows the geometry of plates, the resulting slenderness parameter, and the plate labeling used.

Table 2: Plates geometry

Plate	t	β
P_0	1.25	800
P_1	2	500
P_2	5	200
P_3	8	125
P_4	10	100
P_5	12	83.33

3.1.2 Imperfection influence:

We begin with investigating the effect of initial imperfection on the predicted yield load of plates. Conventionally, imperfection in FEM is applied as a percentage of the first elastic buckling mode, or a combination of the first few modes. We vary both the magnitude of imperfection and number of contributing modes in what follows.

3.1.2.1 Imperfection applied using the first mode only:

For the first set of analyses, we investigate the magnitude of imperfection applied according to the first buckling mode at two different levels of 1% and 5%. Table 3 shows the predicted yield load P_y from the model (FEA) using both these magnitudes. It can be seen that the magnitude of the applied imperfection does not have a significant influence for plates with slenderness ratio of $\beta \leq 200$ as the percentage difference between the predictions is low.

Table 3: P_y (KN) values for P_0, P_2, P_4, P_5 with different imperfection magnitudes based on % of the first buckling mode

	Imperfection%	P_y	
		FEA	Difference
P_0	1	30.98	13.48
	5	27.3	
P_2	1	331.59	1.40
	5	327	
P_4	1	1793.5	0.20
	5	1790	
P_5	1	2395	0.00
	5	2395	

3.1.2.2 1% Imperfection applied using the first two modes:

Next, we fix the imperfection magnitude at 1%, and apply it based on the first two modes. Table 4 shows the results of this study, where it can be seen that the mode number which the imperfection is based on has a significant influence in thin plates. The influence becomes less significant when the plates become thicker.

Table 4: P_y (KN) values for P_0, P_2, P_4, P_5 with 1% imperfection applied in different modes.

	Mode	P_y	
		FEA	Difference
P_0	1	30.98	47.24
	2	21.04	
P_2	1	331.59	0.00
	2	331.6	
P_4	1	1793.5	-4.19
	2	1872	
P_5	1	2395	0.00
	2	2395	

3.1.2.3 Imperfection applied in different number of buckling modes:

For the final set of analyses in this section, we again fix the imperfection at 1%, but apply it based on a combination of modes. Table 5 shows that applying the imperfection in different modes has a significant influence in thin plates. Similar to the previous section, the influence becomes less significant when the plates become thicker.

Table 5: P_y (KN) values for P_0, P_2, P_4, P_5 with 1% imperfection applied in different number of modes.

	No. of modes	P_y	
		FEA	Difference
P_0	1	30.98	35.88
	3	22.8	
P_2	1	331.59	1.71
	3	326	
P_4	1	1793.5	-4.35
	3	1875	
P_5	1	2395	0.00
	3	2395	

These analyses show that the imperfection magnitude and the modes contibuting to it has a somewhat negligible effect on the predicted yeild load (especially for stocky plates). Therefore, we use 1% imperfection applied based on the first mode in the rest of the thesis.

3.1.3 Plates classification:

For this thesis, we define a plate classification scheme based on their yield and buckling load as follows. Plates are considered thin if $P_{cr} < P_y$, stocky plate: if $P_{cr} \gg P_y$ and moderate if $0 < \frac{P_{cr} - P_y}{P_y} * 100 < 10\%$.

Next, we determine the "class" of plate for all plates used in this thesis, and present the results in Table 6. All models are subject to an initial imperfection of 1% (based on the previous section results). Table 6 shows that the behavior of plates change by increasing the plate thickness. We note that theoretical yield loads are not available for thin and moderate plates, because buckling precedes yielding.

Table 6: P_{cr} & P_y loads for $P_0 - P_5$ plates.

Plate	P_{cr}		P_y		$\frac{P_{cr} - P_y}{P_y} * 100$	Class
	FEA	Theoritical	FEA	Theoritical		
P_0	3.60	3.50	30.98	N/A	-88.38	Thin
P_1	14.60	14.20	67.31	N/A	-78.31	Thin
P_2	227.80	221.60	331.59	N/A	-31.30	Thin
P_3	930.00	907.60	982.98	N/A	-5.39	Moderate
P_4	1800.00	1772.70	1793.50	N/A	0.36	Moderate
P_5	3125.00	3063.30	2395.00	2390.20	30.48	Stocky

3.1.3.1 Out of plane displacements at yielding point:

In this subsection, we plot the force versus out-of-plane displacement curves for each plate results shown in the Table 6 to verify the yield and buckling load. We also show the von Mises stress distribution at the yield load magnitude. We begin with showing the force-displacement curve and the von Mises stress distribution for P_0, which are shown in Figure 6. From these, we determine the buckling load as 3.0 KN and yield load as 30.98 KN respectively. The yield load can be verified by observing the left panel of Figure 6, where we see that yielding has started at the tension field. However, the buckling load is estimated at 3.0 KN because this is where the displacement direction has changed in the curve, which suggests that buckling has happened. We observe that for thin plates, yield happened in different regions due to the excessive deformations ($e.g.,\ P_0$). Figures 7, 8, 9 show the force-displacement curve along with the von Mises stress distribution for plates P_1, P_2, P_3 respectively. We observe that when plates get stocky, the yield reign starts to form in the diagonal area, until the yielding happens due the material only (e.g., $P_4\ P_5$). Figures 10, 11 show the force-displacement curve along with the von Mises

stress distribution for plates P_4 and P_5. Another observation is that slender plates (P_0 and P_1) gain stiffness after buckling (the load keeps on increasing), but the stocky plates show a decrease in capacity.

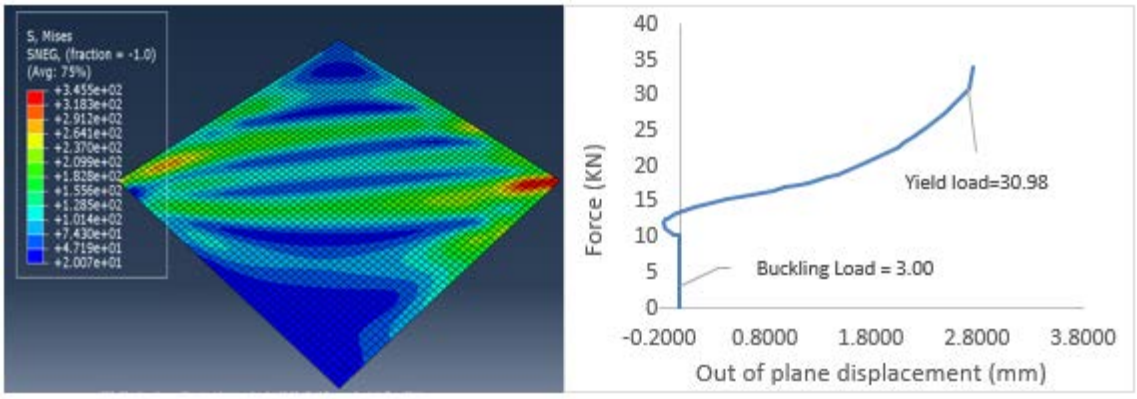

Figure 6: Von Mises stress and Force-displacement chart for P_0

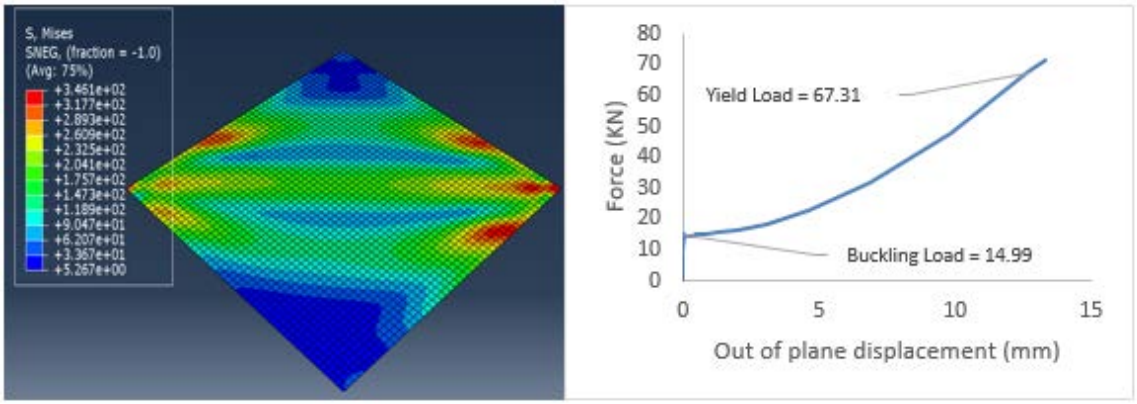

Figure 7: Von Mises stress and Force-displacement chart for P_1

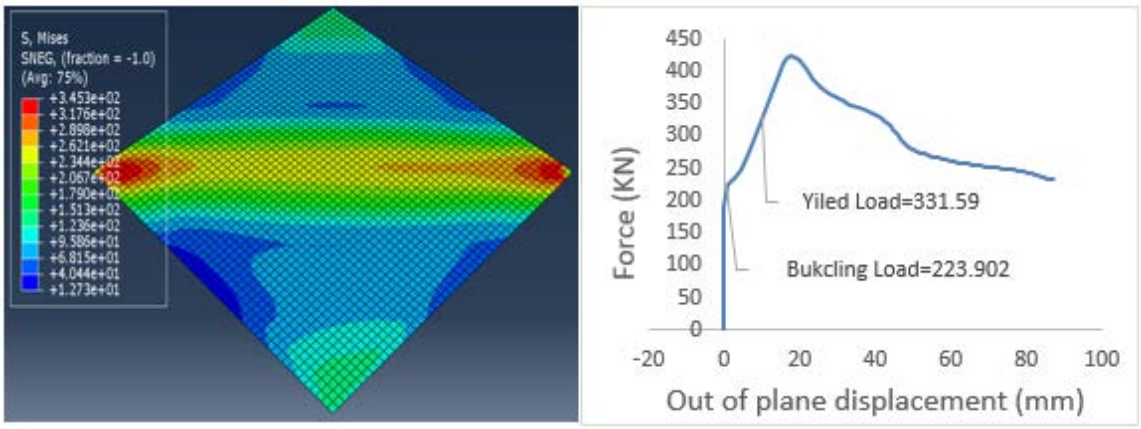

Figure 8: Von Mises stress and Force-displacement chart for P_2

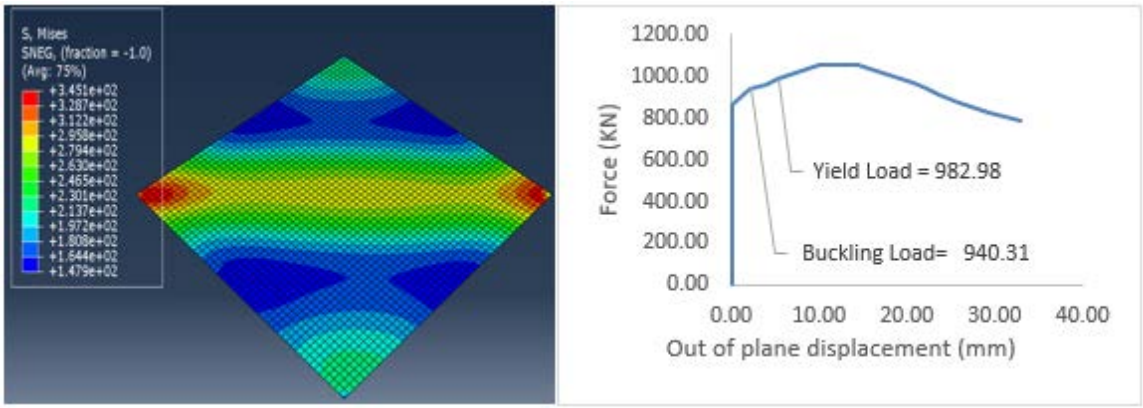

Figure 9: Von Mises stress and Force-displacement chart for P_3

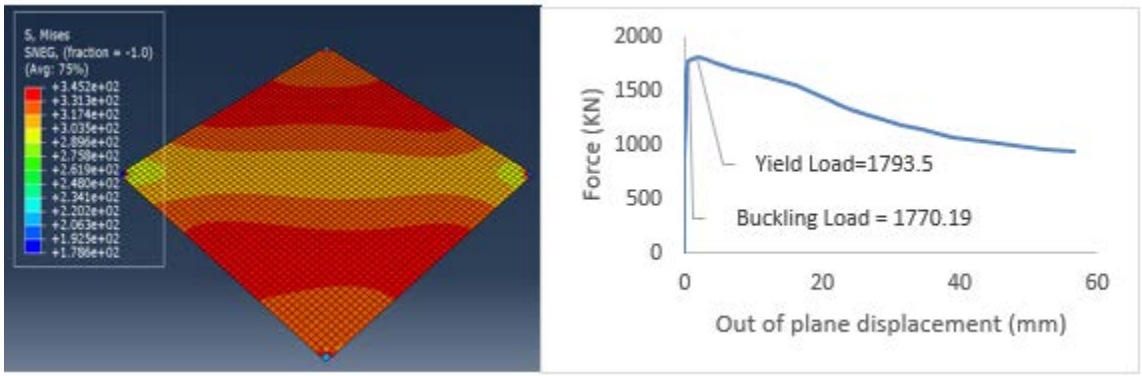

Figure 10: Von Mises stress and Force-displacement chart for P_4

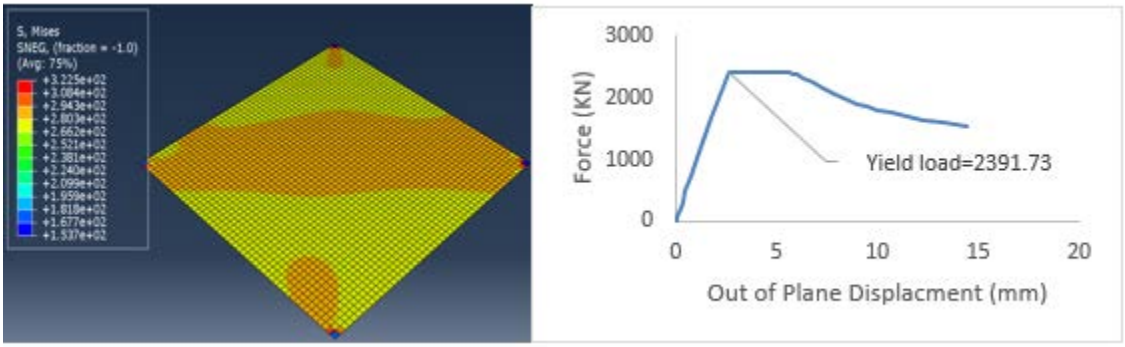

Figure 11: Von Mises stress and Force-displacement chart for P_5

3.2 Plates with stiffeners:

In the next phase of analyses, we added stiffeners to plates and conducted the FEA similar to the procedure described previously.

3.2.1 Plates geometry:

All plates have a thickness of $t_p = 1.25\ mm$ and a stiffener thickness $t_s = 6\ mm$. We then determine h_s using Eq. (10 to 13). Table 7 shows plates geometry.

Table 7 : Plate stiffeners dimensions

Plate	h_s
H0V0	N/A
H1V0	13.15
H2V0	15.63
H3V0	17.06
H1V1	12.05
H2V2	10.75
H3V3	10.48
H4V4	9.89

We again describe the notation used $HxVy$:

x =number of stiffeners in the horizontal direction.

y = number of stiffeners in the vertical direction.

3.2.2 Imperfection influence:

3.2.2.1 Imperfection percentage % applied based on the first mode:

We begin with investigating the effect of initial imperfection on the predicted yield load of stiffened plates. Conventionally, imperfection in FEM is applied as a percentage of the first elastic buckling mode, or a combination of the first few modes. We vary both the magnitude of imperfection and number of contributing modes in what follows. Table 8 shows that number of stiffeners reduces the influence of the applied imperfection.

Table 8: P_y values for $H0V0, H1V0, H3V3$ with different imperfection values

	Imperfection%	P_y	
		FEA	Difference
H0V0	1	30.98	28.15
	5	24.18	
H1V1	1	31.8	2.25
	5	31.1	
H3V3	1	78.55	7.24
	5	73.25	

3.2.2.2 Imperfection 1% applied in different modes:

Next, we fixed the imperfection magnitude at 1 % and applied it based on both the first and second modes. Table 9 shows that applying imperfection in different modes has a significant influence on the yield load. The influence depends on the mode deformation shape.

Table 9: Py values for $H0V0, H1V0, H3V3$ with 1% imperfection applied in different modes.

	Mode	P_y	
		FEA	Difference
H0V0	1	30.98	47.24
	2	21.04	
H1V1	1	31.8	-55.34
	2	71.2	
H3V3	1	78.55	0.19
	2	78.4	

3.2.2.3 Imperfection applied in different number of buckling modes:

Finally, we applied the 1% imperfection based on the first 3 modes and compared the resulting P_y values with the values from applying the imperfection in the first mode only.

Table 10: shows that adding stiffeners reduces the influence until it vanishes.

Table 10: P_y values for $H0V0, H1V0, H3V3$ with 1% imperfection applied in different number of modes

	No. of modes	P_y	
		FEA	Difference
H0V0	1	30.98	35.88
	3	22.8	
H1V1	1	31.8	7.94
	3	29.46	
H3V3	1	78.55	0.19
	3	78.4	

3.2.3 Classification of plates with stiffeners:

3.2.3.1 $t_p = 1.25mm, t_s = 6mm$:

We classify the plates with stiffeners in this section similar to the procedure described in the preceding sections. We begin with $t_p = 1.25mm$ and $t_s = 6m$m. The plate without stiffeners was classified as slender in the preceding sections. We also note that all

plates are subjected to 1% imperfection based on the first mode in accordance with the results of the preceding section. First, we show the buckling shape at the first mode, then we ploted the force versus out-of-plane displacement curves for each plate.

Table 11: shows that adding stiffeners increases the plates overall efficiency by reducing the difference between buckling load and yielding load. However, the overall plate class could not be changed to stocky. We therefore, investigated these models more thoroughly in the next subsection

Table 11: Studied plates Pcr and Py values

Plate	H0V0	H1V0	H2V0	H3V0	H1V1	H2V2	H3V3	H4V4
h_s	N/A	13.15	15.63	17.06	12.05	10.75	10.48	9.98
P_{cr}	3.57	9.67	19.00	33.06	13.83	30.78	58.02	83.30
P_y	30.98	33.45	47.90	55.44	31.80	53.07	78.55	88.26
βsub panel	800.00	400.00	266.67	200.00	400.00	266.67	200.00	160.00
$\frac{P_{cr}-P_y}{P_y} * 100$	-88.48	-71.09	-60.33	-40.37	-56.51	-42.00	-26.14	-5.62

3.2.3.1.1 First mode buckling shape:

To understand why the plate class could not be changed to stocky using stiffeners, we present the first buckling mode of the plates shown in Table 7 in Figures 12 to 19. It appears that adding stiffeners divided the plate to almost independent sub-plates, and when the difference between buckling and yielding loads is relatively high, every sub plate has its own buckling shape which is similar to a plate without any stiffeners (e.g., $H1V1$).

When the difference between buckling and yield load becomes smaller, stiffeners lose their effect as a support and the plate has one buckling shape (e.g., $H3V3$ and $H4V4$).

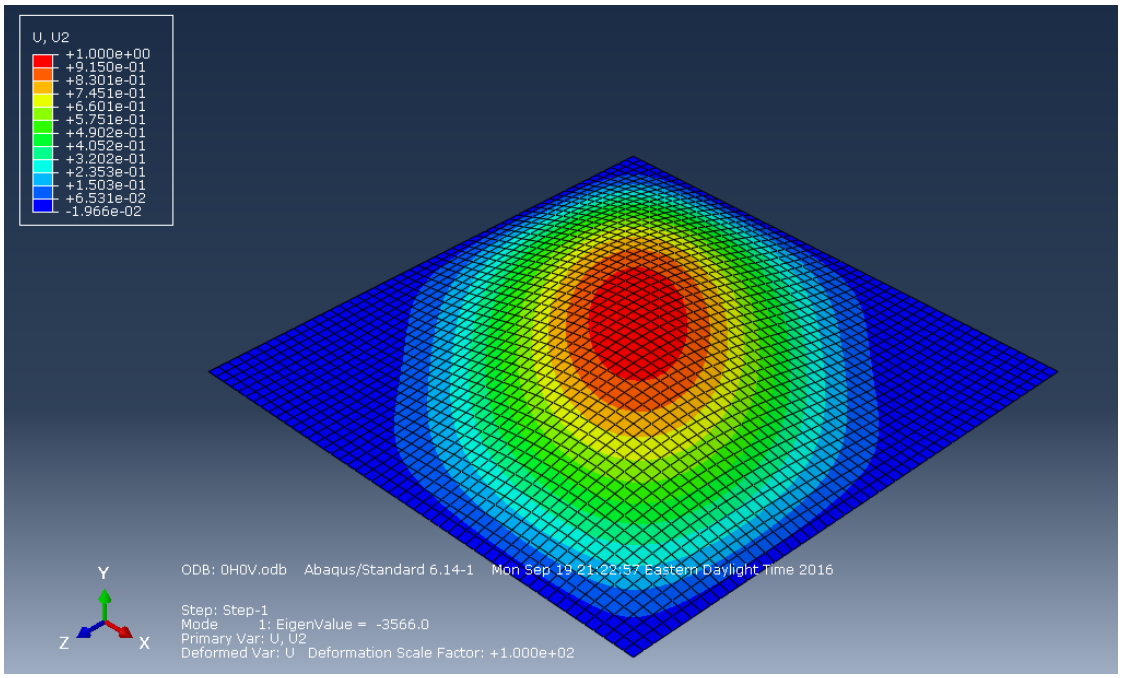

Figure 12: Eigen mode for $H0V0$ Plate

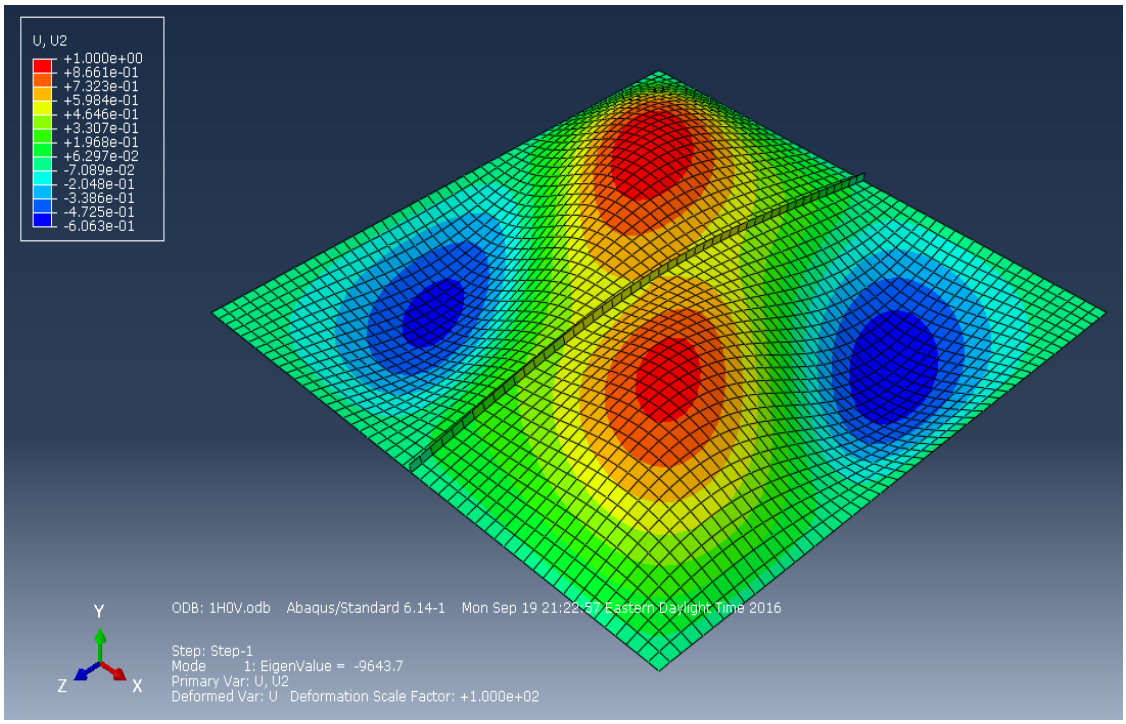

Figure 13: Eigen mode for $H1V0$ Plate

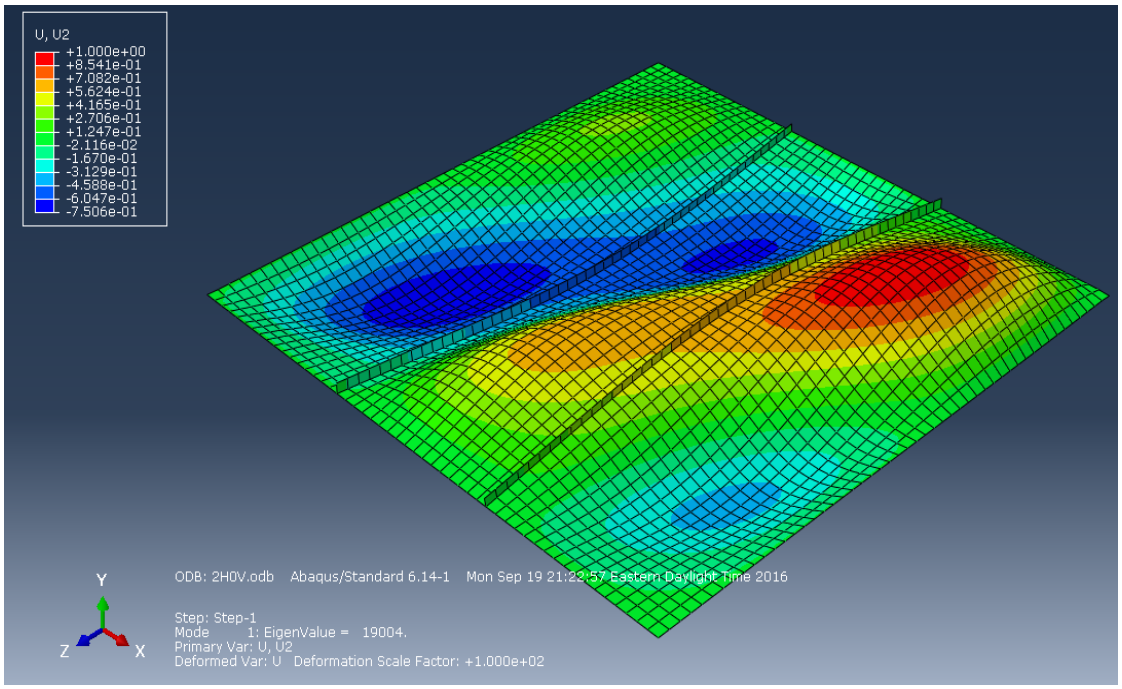

Figure 14: Eigen mode for $H2V0$ Plate

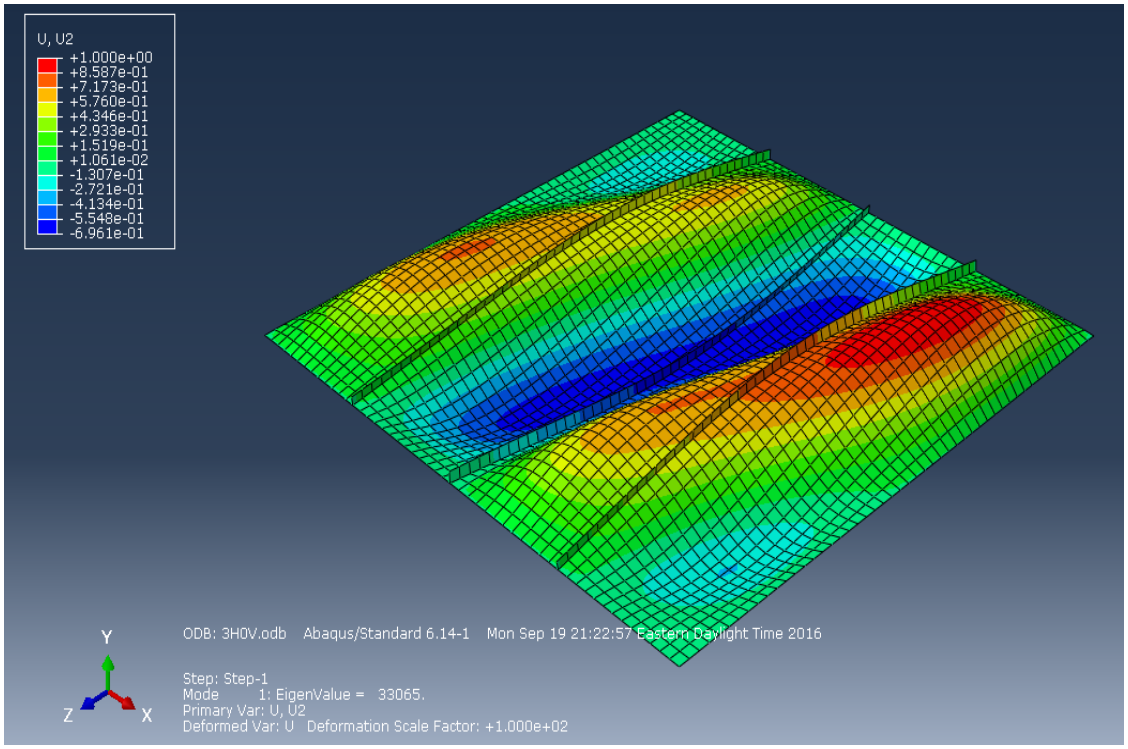

Figure 15: Eigen mode for $H3V0$ Plate

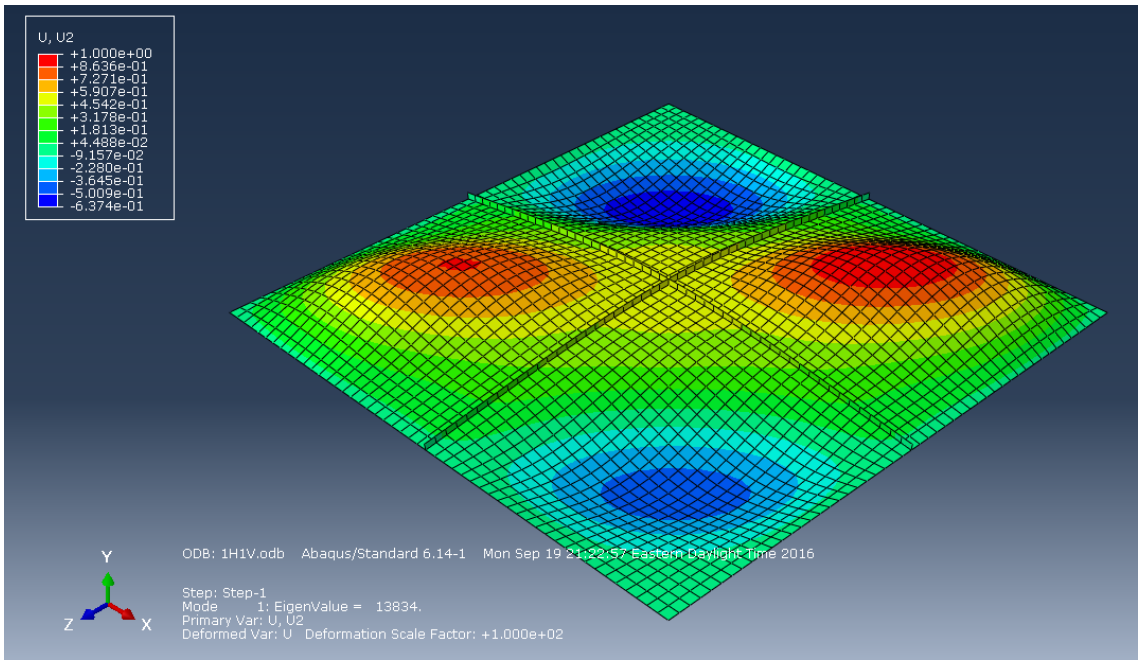

Figure 16: Eigen mode for $H1V1$ Plate

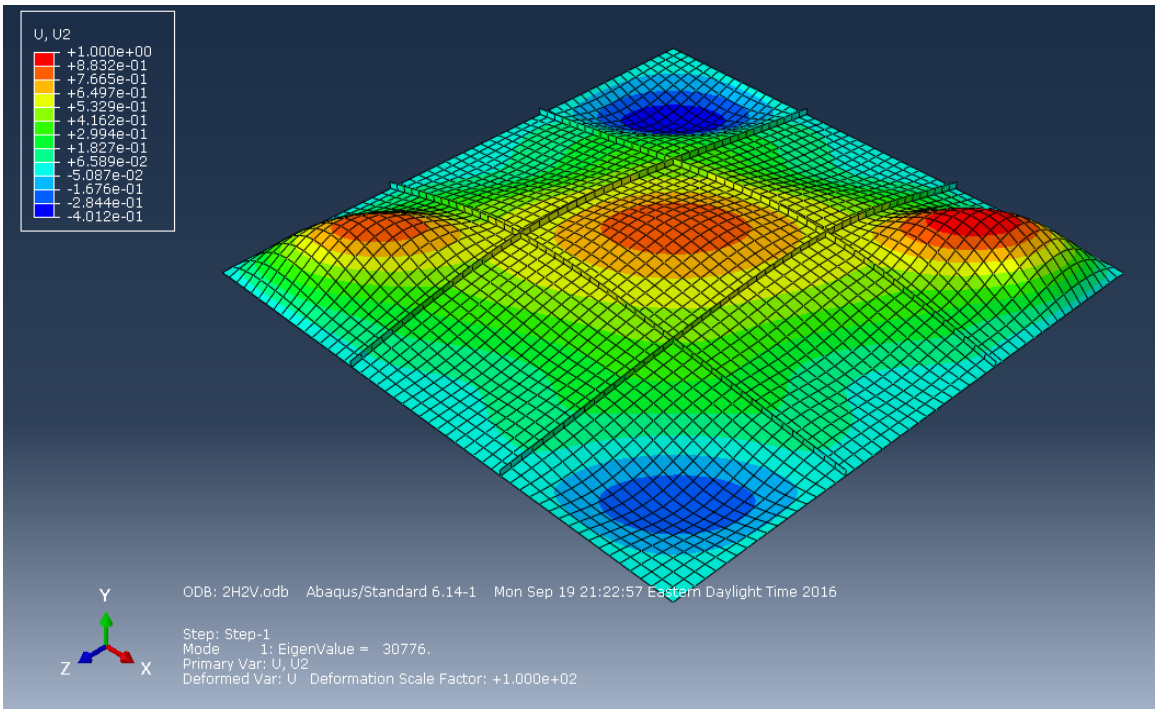

Figure 17: Eigen mode for $H2V2$ Plate

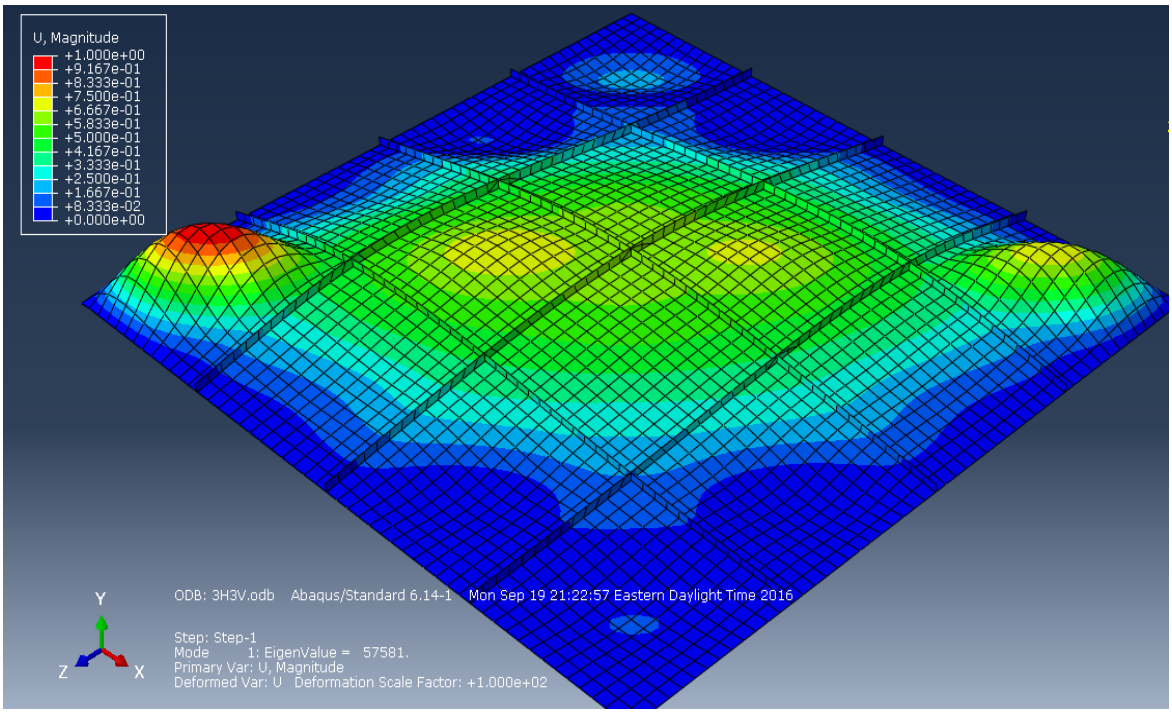

Figure 18: Eigen mode for $H3V3$ Plate

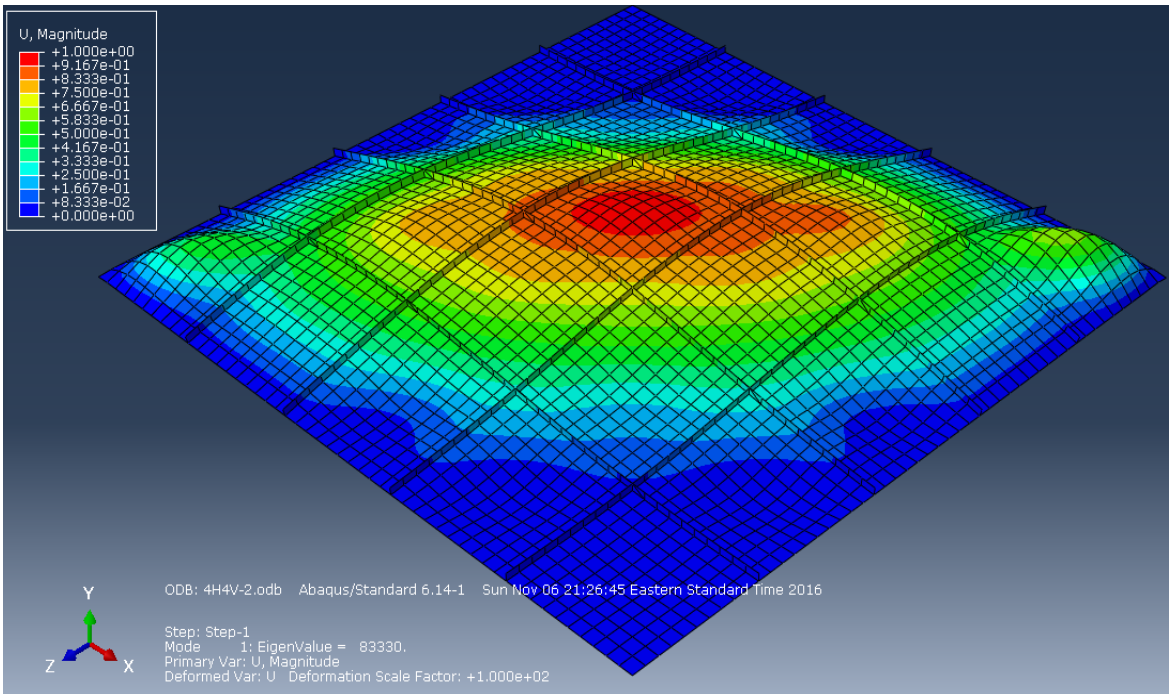

Figure 19: Eigen mode for $H4V4$ Plate

3.2.3.1.2 Out of plane displacements at yielding point:

Figures 20 to 26 show von Mises stress and force-displacement plot for plates with stiffeners. As we discussed for buckling shapes in first modes, stress distribution shows that when plate is thin, every sub plate has its own stress distribution as an independent plate (e.g., $H2V2$). When the plate becomes closer to stocky behavior, stress distribution becomes more uniform for the whole plate (e.g., $H4V4$).

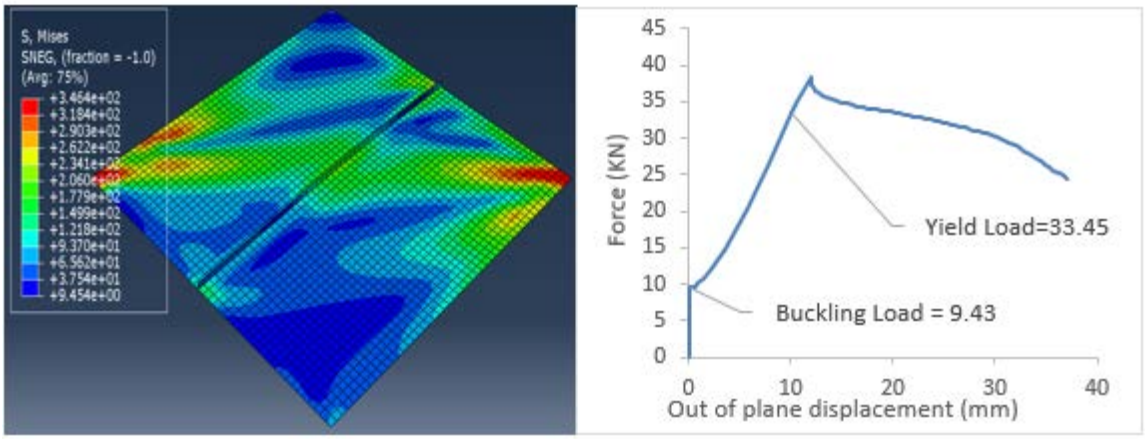

Figure 20: Von Mises stress and force-displacement plot for $H1V0$

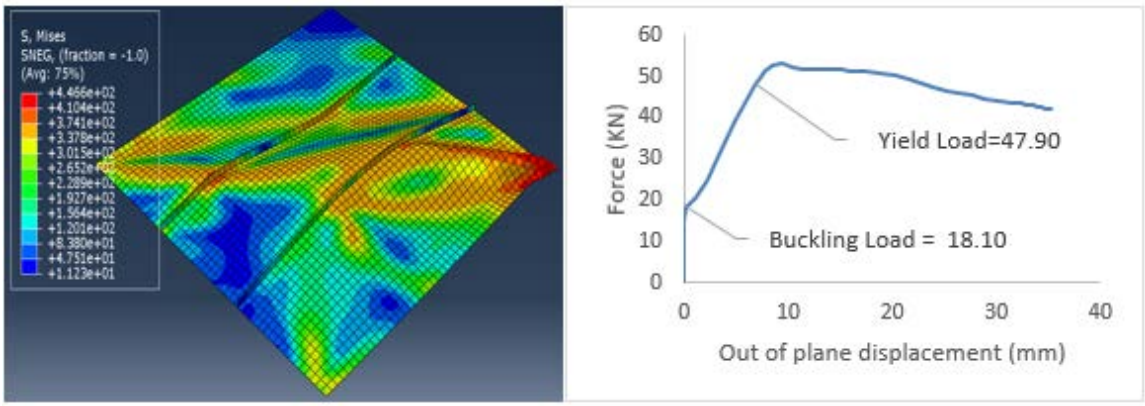

Figure 21: Von Mises stress and force-displacement plot for $H2V0$

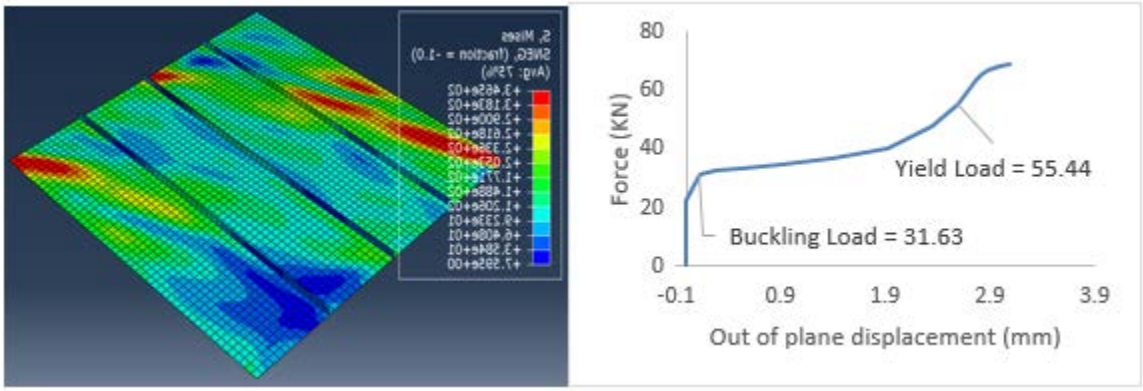

Figure 22: Von Mises stress and force-displacement plot for $H3V0$

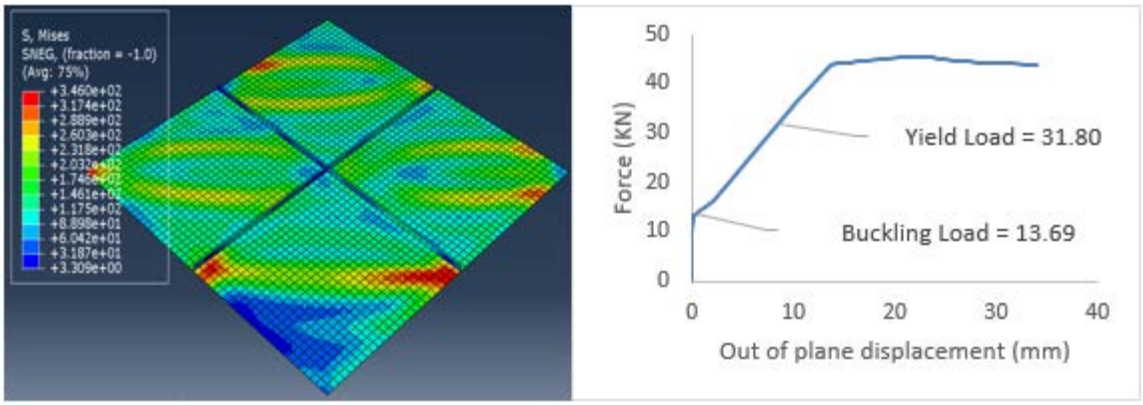

Figure 23: Von Mises stress and force-displacement plot for $H1V1$

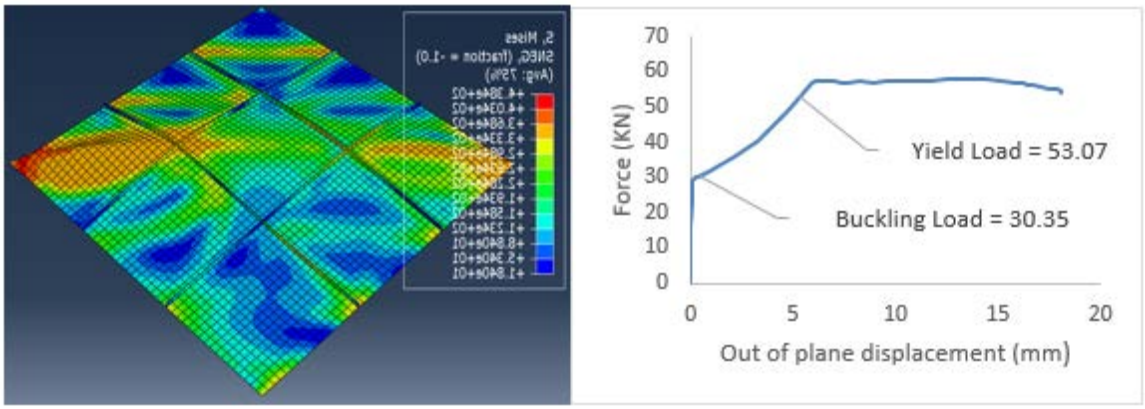

Figure 24: Von Mises stress and force-displacement plot for $H2V2$

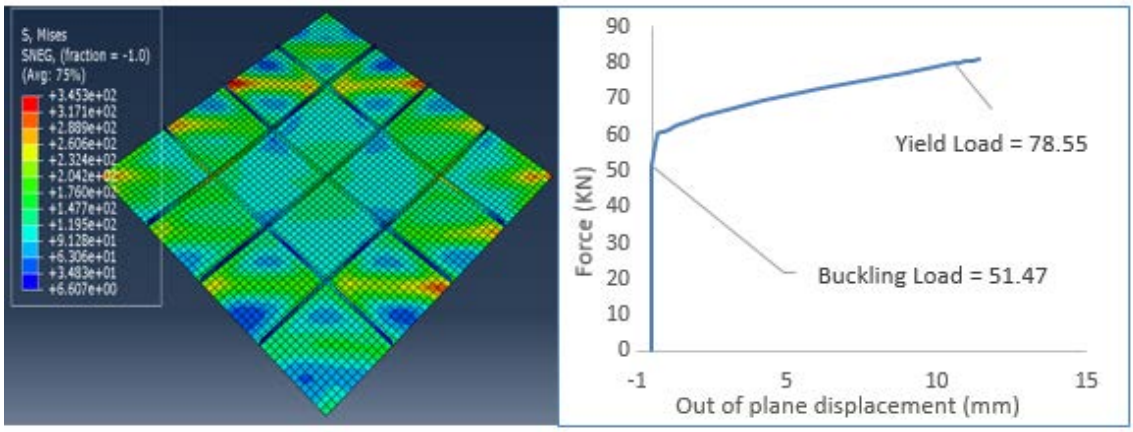

Figure 25: Von Mises stress and force-displacement plot for $H3V3$

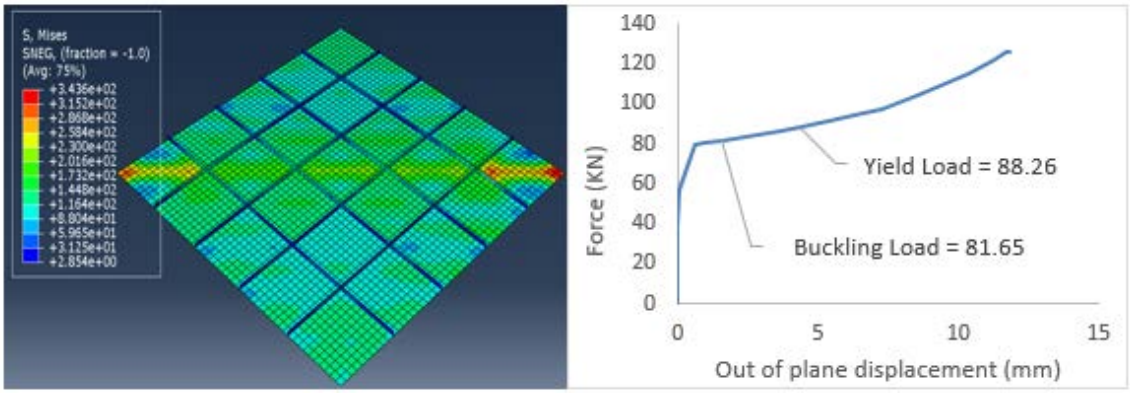

Figure 26: Von Mises stress and force-displacement plot for $H4V4$

Because even adding 8 stiffeners to a plate with $t_p = 1.25\ mm$ did not change the plate overall behavior, another plate with $t_p = 5\ mm$ thickness was analyzed. The stiffeners thickness and heights were calculated using Eq. (8) to (13). Stiffener thickness was chosen as $t_s = 20\ mm$.

3.2.3.2 Analysis on a plate with $t_p = 5\ mm$, and stiffener thickness of $t_s = 20\ mm$:

We did the same analysis as before on this plate. Table 12 shows the results. This table shows that the plate behavior has not changed after adding 2 stiffeners in the same

direction. After adding more stiffeners, a local yielding happened between the stiffeners due the high stiffness of the stiffeners which prevents yielding to spread through the plate. Therefore, a plate with the same thickness and less stiffener thickness was modeled.

Table 12: Studied plates Pcr and Py values

Plate	H0V0	H1V0	H1V1
h_s	0.00	29.58	30.25
P_{cr}	227.81	542.00	882.32
P_y	331.59	915.00	1590.00
βsub panel	800.00	400.00	400.00
$\frac{P_{cr}-P_y}{P_y}*100$	-31.30	-40.77	-44.51

3.2.3.3 Analysis on a plate with $t_p = 5\ mm$, and stiffener thickness of $t_s = 10\ mm$

This plate is again analyzed with a similar procedure. Table 13 summarizes the results of this phase. This Table shows that the behavior of the plate was changed from slender to stocky after adding two stiffeners ($H2V0$). However, adding more stiffeners caused a local yielding.

Table 13: Studied plates Pcr and Py values

Plate	H0V0	H1V0	H2V0	H1V1
h_s	N/A	41.83	49.50	40.00
P_{cr}	277.81	595.78	1004.60	874.04
P_y	331.59	652.00	758.50	864.50
βsub panel	800.00	400.00	266.67	400.00
$\frac{P_{cr}-P_y}{P_y}*100$	-16.22	-8.62	32.45	1.10

3.2.3.3.1 Out of plane displacements at yielding point:

Figures 27 to 29 show von Mises stress and force-displacement plot for $H1V0, H1V1, H2V0$ plates.

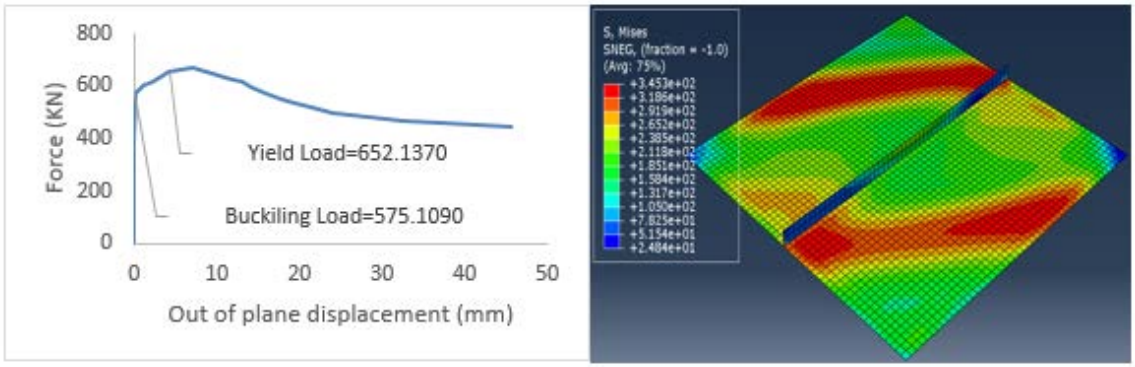

Figure 27 : Von Mises stress and force-displacement plot for $H1V0$

Figure 28 shows that after the yield load, plates lose their stiffness considerably. This may have occurred due to simultaneous occurrence of yielding and buckling.

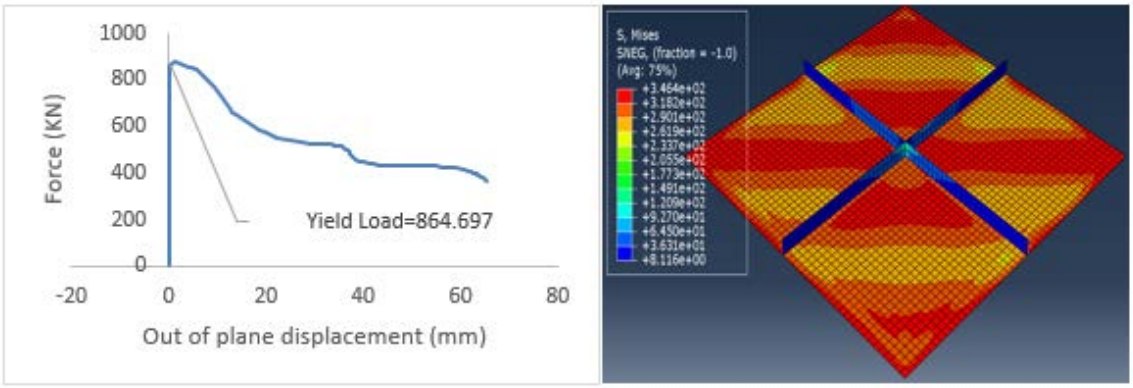

Figure 28: Von Mises stress and force-displacement plot for $H1V1$

Figure 29 shows that after yielding, an increase in displacment happened without an increase in the applied load, which is consistent with the yielding zone, and shows that the plastic buckilng regime is started.

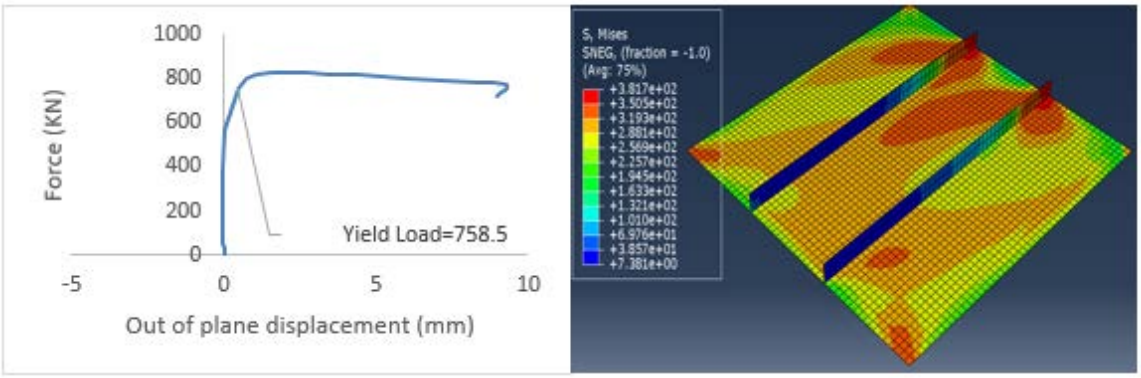

Figure 29: Von Mises stress and force-displacement plot for $H2V0$

CHAPTER IV

CONCLUSION AND FUTURE DIRECTION

4.1 Concluding remarks:

In this thesis, a numerical investigation of shear plates' behavior with and without stiffeners was performed. All analyses were static, and boundary conditions were chosen so that a state of pure shear could be achieved as close as possible. A total of 42 plates were modeled, out of which 12 models were used to classify the plates into either: slender, moderate and stocky based on their yield and buckling loads. The other 30 models were used to study the effect of adding stiffeners on the plate behavior. An initial imperfection was applied to all models to initiate buckling in the nonlinear geometric Riks analysis. The imperfection magnitude was chosen as 1% of the first buckling mode after extensive numerical investigation. The stiffeners were designed based on the procedure described in (Alinia & Sarraf Shirazi 2009).

It was found that, in general, the force-displacement plots for thin plates had three consecutive stages:1- before buckling,

2- buckling stage

3- after yielding. As an example, the reader is referred to Figure 7 .

The study shows that when the stiffeners are added to a thin plate the second stage shrinks which increases the plate efficiency until this stage disappears and the yielding happens before buckling, under which situation the plate could be classified as stocky (thick) plate. Figure 29 shows a typical force-displacement plot for a stocky plate.

The models in this study showed that behavior of plates could be changed by adding stiffeners from slender to stocky. This was desirable because buckling which was a sudden failure was delayed to after yielding. However, these results also showed that the correct design of stiffeners had a critical influence in changing the plate behavior. Our study showed that depending on the stiffener thickness, the stiffeners might cause a local yielding, and the plate became sub-divided for too thick of stiffeners. Therefore, choosing a moderate value for stiffener thicknesses t_s from Eq.(8) is recommended.

In conclusion, adding stiffeners could enhance the plate overall performance by changing its behavior from slender to moderate to stocky plate without adding a lot of material. Moreover, adding stiffeners in the same direction produces better results than adding the same number of stiffeners in both plate directions. The study shows also that the imperfection magnitude has more effect on thin plates. However, it loses its effect by adding stiffeners. Also, Imperfection amount applied in different buckling modes has a significant effect on the yield load and it depends on the buckling mode shape.

4.2 Future directions:

Our study was limited to square plates, static load and simply supported boundary conditions. Therefore, further studies should be held to study the effect of adding

stiffeners with different load and geometry conditions. Also, our research showed that stiffeners design equations need further investigations to add more specific recommendation to design stiffeners effectively.

REFERENCES

[1]. Alinia, M. M., & Dastfan, M. (2006). Behaviour of thin steel plate shear walls regarding frame members. Journal of Constructional Steel Research, 62(7), 730–738.

[2]. Amani, M., Alinia, M. M., & Fadakar, M. (2013). Imperfection sensitivity of slender/stocky metal plates. Thin-Walled Structures, 73, 207–215.

[3]. Chen, S. J., & Jhang, C. (2006). Cyclic behavior of low yield point steel shear walls. Thin-Walled Structures, 44(7), 730–738.

[4]. Deb, A., & Booton, M. (1988). Finite element models for stiffened plates under transverse loading. Computers and Structures, 28(3), 361–372.

[5]. Gheitasi, A., & Alinia, M. M. (2010). Slenderness classification of unstiffened metal plates under shear loading. Thin-Walled Structures, 48(7), 508–518.

[6]. Wang, C. M., Chen, Y., & Xiang, Y. (2004). Plastic buckling of rectangular plates subjected to intermediate and end inplane loads. International Journal of Solids and Structures, 41(16–17), 4279–4297.

[7]. Wang, C. M., Xiang, Y., & Chakrabarty, J. (2001). Elastic/plastic buckling of thick plates. International Journal of Solids and Structures, 38(48–49), 8617–8640.

[8]. Zirakian, T., & Zhang, J. (2015). Buckling and yielding behavior of unstiffened slender, moderate, and stocky low yield point steel plates. Thin-Walled Structures, 88, 105–118.

[9]. Alinia, M. M., Gheitasi, A., & Erfani, S. (2009). Plastic shear buckling of unstiffened stocky plates. Journal of Constructional Steel Research, 65(8–9), 1631–1643.

[10]. Novoselac, S., Ergić, T., & Baličević, P. (2012). Linear and Nonlinear Buckling and Post Buckling Analysis of a Bar with the Influence of Imperfections. Tehnički Vjesnik, 19(3), 695–701.

[11]. Sanal, O., & Gunay, E. (2008). Finite Element Buckling Analyses of Transversely Stiffened Orthotropic Rectangular Thin Plates under Shear Loads. Journal of Reinforced Plastics and Composites, 28(1), 109–127.

[12]. Tetsuro, I., & Ben, K. (1993). Analysis of plastic buckling of steel plates. International Journal of Solids and Structures, 30(6), 835–856.

[13]. Alinia, M. M., & Sarraf Shirazi, R. (2009). On the design of stiffeners in steel plate shear walls. Journal of Constructional Steel Research, 65(10–11), 2069–2077.

[14]. Abaqus 6.12 :Abaqus CAE User's Manual. (2012). Abaqus CAE User's Manual. Dassault Systèmes Simulia, 1174.

[15]. Abaqus 6.12: Analysis User's Manual Volume 2: Analysis. (2012). Analysis User's Manual Volume 2: Analysis. Dassault Systèmes Simulia (Vol. II).

[16]. Abaqus 6.12: Getting Started with Abaqus: Interactive Edition. (2012). Getting Started with Abaqus: Interactive Edition. Simulia.

[17]. Gerstle, K. H. (2001). Advanced Mechanics of Materials. Journal of Structural Engineering (Vol. 127).

[18]. Abaqus 6.12: Analysis User's Manual Volume 4: Elements. (2012). Analysis User's Manual Volume 4: Elements. Dassault Systèmes Simulia (Vol. IV).

[19]. Zhao, M. (2008). On Nonlinear Buckling and Collapse Analysis using Riks Method. Abaqus Users' Conference, 1–9.

[20]. Taczała, M., Buczkowski, R., & Kleiber, M. (2017). Nonlinear buckling and post-buckling response of stiffened FGM plates in thermal environments. Composites Part B: Engineering, 109, 238–247.

[21]. Paik, J. K., & Seo, J. K. (2009). Nonlinear finite element method models for ultimate strength analysis of steel stiffened-plate structures under combined biaxial compression and lateral pressure actions-Part II: Stiffened panels. Thin-Walled Structures, 47(8–9), 998–1007.

[22]. Paulo, R. M. F., Teixeira-Dias, F., & Valente, R. A. F. (2013). Numerical simulation of aluminium stiffened panels subjected to axial compression: Sensitivity analyses to initial geometrical imperfections and material properties. Thin-Walled Structures, 62, 65–74.

[23]. Sabouri-Ghomi, S., Ventura, C. E., & Kharrazi, M. H. (2005). Shear Analysis and Design of Ductile Steel Plate Walls. Journal of Structural Engineering, 131(6), 878–889.

[24]. Wang, W., Guo, S., Chang, N., & Yang, W. (2010). Optimum buckling design of composite stiffened panels using ant colony algorithm. Composite Structures, 92(3), 712–719

[25]. De Souza Neto, E. A., & Feng, Y. T. (1999). On the determination of the path direction for arc-length methods in the presence of bifurcations and “snap-backs.” Computer Methods in Applied Mechanics and Engineering, 179(1–2), 81–89.